



24 trench at four distances from the drain: 0.6 m, 1.1 m, 2.1 m and 4.0 m. In the E&Bt horizon, four  
25 different soil volumes (ochre, pale brown, white-grey and black) were sampled at all four distances  
26 from the drain. Furthermore, we analyzed soil solutions sampled with piezometer, porous cups,  
27 and at the drain outlet. The Cu concentrations were lowest in the surface (Ap) horizons (6.5-8.5  
28  $\mu\text{g g}^{-1}$ ) and increased with depth to the clay-rich Bt horizons (10.5-12  $\mu\text{g g}^{-1}$ ), because of clay  
29 eluviation and associated Cu transport. The  $\delta^{65}\text{Cu}$  values significantly decreased from the surface  
30 (Ap =  $-0.25 \pm 0.07$  ‰) to the deeper horizons, but show no significant variation among the deeper  
31 horizons ( $-0.41 \pm 0.28$  ‰) and no correlation with the clay content, indicating that clay eluviation  
32 does not significantly affect  $\delta^{65}\text{Cu}$  values. The isotopically heavier  $\delta^{65}\text{Cu}$  values in the Ap horizons  
33 can probably be explained by agricultural management practises like sludge application and  
34 fertilization. Close to the drain (position 0.6 m), Cu concentrations were depleted and the lighter  
35 Cu isotope was enriched ( $-0.91 \pm 0.15$  ‰) in the uppermost part of the E&Bt horizon. We attribute  
36 this to the changing redox conditions, caused to lowering of the water level close to the drain.  
37 Copper concentrations in black and ochre volumes were significantly higher than in pale-brown  
38 and white-grey volumes. The black volume had significantly higher  $\delta^{65}\text{Cu}$  values than the ochre  
39 volume indicating preferential sorption/occlusion of the heavy Cu isotope by Fe oxides. Enhanced  
40 clay eluviation in bulk soil close to the drain and in specific soil volumes did not affect  $\delta^{65}\text{Cu}$   
41 values. Cu concentrations ( $2.1 - 14 \mu\text{g L}^{-1}$ ) and  $\delta^{65}\text{Cu}$  ( $0.04 - 0.42$  ‰) values in water samples  
42 showed no clear relation with redox changes along the trench perpendicular to the drain. The  
43 enrichment of the heavy Cu isotope in the solution samples ( $\Delta^{65}\text{Cu}_{(\text{soil-solution})} = -0.61 \pm 0.41$ )  
44 indicates that reductive Cu mobilization is not the main driver of Cu leaching, because this would  
45 preferentially mobilize isotopically light Cu. We conclude that the eluviation of the  $<2\mu\text{m}$  fraction,  
46 strongly controlled Cu concentrations, but had no discernible effect on  $\delta^{65}\text{Cu}$  values. The changing

47 redox conditions did not seem to control Cu concentrations and the stable isotope distribution in  
48 most of the bulk soil, soil volumes and soil water. Instead, weathering, complexation of leached  
49 Cu, Cu application with fertilizers and sorption processes within the soil controlled its  $\delta^{65}\text{Cu}$   
50 values.

51

52 Keywords: Copper isotopes; Lessivation; Redox conditions; Retisol; Soil volumes; drainage; soil  
53 water.

54

## 55 **1. Introduction**

56 In temporal or permanently water-saturated soils, episodic anoxic redox conditions couple  
57 back to many soil chemical properties and may cause mobilization and redistribution of redox-  
58 sensitive elements like Cu. Copper is of interest because of its nutritional importance as well as  
59 pollution risk. Furthermore, the redox behavior of Cu is assumed to play an important role in  
60 colloidal mobilization of a number of toxic elements like Ag, Cd, Hg and Pb (Abgottspon et al.,  
61 2015; Hofacker et al., 2013; Weber et al., 2009a). Thus, information about Cu behavior in  
62 temporarily water-saturated soils and the response of Cu to changes in the soil water regime might  
63 help to understand the release mechanisms of redox-sensitive trace elements.

64 When soils get waterlogged, the redox potential drops and Fe and Mn (oxyhydr)oxides are  
65 dissolved releasing associated trace elements (e.g., As, Ba, Co, Cr, V; Abgottspon et al., 2015; Du  
66 Laing et al., 2009; Sipos et al., 2011). Changes to anoxic conditions may cause microbial formation  
67 of reduced metal ( $\text{Cu}^+$  and  $\text{Cu}[0]$ ) colloids (Weber et al., 2009b). When the redox potential drops  
68 sufficiently, microbial sulfate reduction is initialized and the mobility of Cu can be limited by the  
69 formation of or co-precipitation with sulfides (Weber et al., 2009b; Borch et al., 2010). However,

70 sulfate reduction may also favor the release of Cu-sulfide colloids into soil solution, resulting in  
71 enhanced mobility during several days after flooding (Abgottspon et al., 2015; Hofacker et al.,  
72 2013; Weber et al., 2009a). When the conditions in the soil change to oxic, Cu(0) is rapidly  
73 oxidized to  $\text{Cu}^{2+}$ , while  $\text{Cu}^+\text{-S}_{\text{org}}$  or  $\text{Cu}_x\text{S}$  is only slowly oxidized limiting Cu solubility in soil  
74 (Fulda et al., 2013b). Balint et al. (2014) confirmed that Cu leaching decreased over four redox  
75 cycles, which they attributed to the redistribution of Cu from labile to more recalcitrant chemical  
76 fractions in soil.

77         Several soil processes result in fractionation of Cu isotopes (Fig. 1, Bigalke et al., 2010a;  
78 c; 2011; 2013). Sorption of Cu to Al and Fe (oxyhydr)oxides caused an enrichment of heavy Cu  
79 on the surface of the Fe (oxyhydr)oxides (Balistrieri et al., 2008; Pokrovsky et al., 2008). Sorption  
80 to organic ligands shows different fractionation factors depending on the type of organic ligand  
81 and pH (Bigalke et al., 2010b; Ryan et al., 2014). Lighter Cu isotopes are preferentially adsorbed  
82 on clay mineral surfaces (Li et al., 2015). Redox reactions cause pronounced fractionation, leaving  
83 the reduced Cu species enriched in lighter Cu isotopes (Ehrlich et al., 2004; Zhu et al., 2002).  
84 Babcsányi et al. (2014) and Bigalke et al. (2010a; 2011; 2013) found temporally water-saturated  
85 soil horizons and wetlands to be enriched in heavy Cu isotopes, which they attributed to the loss  
86 of light Cu by leaching of reduced colloidal Cu forms. Liu et al. (2014a) studied weathering and  
87 soil formation under different climatic conditions and attributed variations in the isotopic  
88 composition to sorption of Cu to organic carbon in soils and leaching of heavy Cu, while also  
89 different redox conditions in the soils may have caused significant fractionation. In oxic weathered  
90 soils, leaching of heavy Cu because of complexation and downward transport with humic acids  
91 was also described by Bigalke et al. (2011). Fekiacova et al. (2015) recently compiled data from  
92 contaminated and uncontaminated soils and found that contaminated soils tended to show heavier

93  $\delta^{65}\text{Cu}$  values. In addition, fractionations associated with plant uptake of Cu (Jouvin et al., 2012;  
94 Navarrete et al., 2011; Ryan et al., 2013; Weinstein et al., 2011) might affect Cu isotope  
95 distribution in the organic and surface horizons (Bigalke et al., 2011). The literature reveals that  
96 the determination of Cu stable isotope ratios may be a valuable additional tool to mass budgeting  
97 approaches for the identification of the processes by which Cu responds to pedogenesis (e. g., clay  
98 redistribution and redox changes). To study the interaction of the latter two processes, Retisols are  
99 a model soil type.

100         Retisols are characterized by the eluviation of clay from the surface horizons (E horizon)  
101 and transport and accumulation of the clay in deeper horizons (Bt horizon). The subsoil clay  
102 accumulation impedes drainage and leads to temporary water saturation in winter. In such soils,  
103 the combination of eluviation and redox processes is responsible for the morphological  
104 degradation of the soil and the formation of the E&Bt-horizon, characterized by the juxtaposition  
105 of four soil volumes differing in texture and color. To improve agricultural suitability, many  
106 Retisols have been drained (FAO, 2001; IUSS Working Group WRB, 2014). Artificial drainage  
107 was demonstrated to induce i) an increasing intensity of the eluviation process in the immediate  
108 vicinity of the drains and ii) the transport of dissolved Fe and Mn towards the drain lines where  
109 more oxidative conditions favored the precipitation of Fe and Mn oxides in various forms of black  
110 concretions and impregnations (Montagne et al., 2008).

111         We focus on the Cu isotopic composition of soil samples collected from four soil profiles  
112 located at increasing distance from a drain and the evolution of the  $\delta^{65}\text{Cu}$  values of four soil  
113 volumes in the E&Bt horizon as response to the drainage. We aim to answer the following  
114 questions:

- 115 1) What is the effect of clay eluviation and accumulation in the Bt horizons on Cu  
116 concentrations and  $\delta^{65}\text{Cu}$  values?
- 117 2) What is the effect of drainage and associated changes in soil chemistry on Cu  
118 concentrations and  $\delta^{65}\text{Cu}$  values?
- 119 3) How do redox and eluviation processes effect Cu concentrations and  $\delta^{65}\text{Cu}$  values of  
120 soil solutions?  
121

## 122 **2. Materials and methods**

### 123 **2.1. Site description and soil sampling**

124 The study site is located on the crest of Yonne plateau in France where Retisols developed  
125 on quaternary loamy deposits overlying an Eocene clay layer. The deposit contains 70-90% of silt  
126 and 5-20% of clay. The soil was extensively cultivated for at least 200 years. Since 1988, an  
127 artificial subsurface drainage was installed at 1 m depth. The drain spacing was 15 m between  
128 parallel drainage pipes. The soil water regime fluctuates seasonally with saturation from December  
129 or January to February or March depending on the year. The temporary water table possibly  
130 reaches to the A horizon and is lowered close to the drain (Fig. 2; Montagne et al., 2008).

131 Details of the soil sampling procedure are available in Montagne et al. (2008). Briefly, in  
132 2004, i.e. 16 yr after installation of the drainage, soil profiles were sampled from a trench  
133 perpendicular to one drain at four different positions with increasing distance to the drain (0.6, 1.1,  
134 2.1 and 4.0 m, respectively). At each position, bulk soil samples were collected from three soil  
135 horizons (Ap/E&Bt/Bt). The Ap horizon (0 to ~ 30-35 cm depth) has a silty texture and is enriched  
136 with organic matter ( $7.3 \pm 0.3 \text{ g kg}^{-1}$  organic C; Montagne et al., 2008). The E&Bt horizon (~35 to  
137 60 cm depth), shows pronounced eluviation and redoximorphic features resulting in the

138 juxtaposition of four volumes differing in texture and color. The four soil volumes include white-  
139 grey, pale-brown, ochre and black volumes (Montagne et al. 2008). The white-grey and the pale-  
140 brown volumes are most abundant in the E&Bt-horizon, while in the underlying clay-enriched Bt  
141 horizon of yellowish brown color (~55 to ~105 cm depth), the ochre soil volume is by far most  
142 abundant. Soil pH increased with depth from  $7.6\pm 0.1$  in the Ap horizon to  $8.0\pm 0.8$  in the Bt  
143 horizon. In addition to the bulk soil samples, soil monoliths (approximately 27x15x12 cm) were  
144 extracted from the E&Bt horizons at all four distances to the drain. In these monoliths, the white-  
145 grey, pale-brown and ochre soil volumes were manually separated from each other, while black  
146 concretions and impregnations were sorted by wet sieving and the help of a magnetic separation  
147 technique (Montagne et al., 2008).

148 Piezometers were installed at three positions (at 0.7, 1.5 and 4.0 m, respectively, from the  
149 drain) in the E&Bt horizons and porous cups (1 x 2 cm-large) were placed in both, the ochre and  
150 white-grey volumes. In addition, water was collected at the outlet of the main drain of the plot with  
151 an automatic collector. Water samples were collected once a week during the years 2005 and 2006,  
152 and once every two weeks during the two following years. The Eh, pH and temperature were  
153 measured in the field. In the lab, all soil water samples were filtered through a 0.2- $\mu$ m cellulose  
154 filter, acidified with suprapur HNO<sub>3</sub> and stored at 4°C for Fe analysis. Soil water samples were  
155 bulked to obtain a sufficient mass of Cu for isotope analysis. Bulking was done for the three  
156 different water types separately (piezometer, porous cup, and drain water samples) for two  
157 different time periods (2005/06 and 2007/08) resulting in seven different soil water samples. The  
158 water samples were classified according to their Fe concentrations as indicator of redox conditions  
159 in the soil. The Fe concentrations under oxic condition (Eh > 300 mV) were always lower than 40

160  $\mu\text{g L}^{-1}$ . Therefore,  $40 \mu\text{g L}^{-1}$  Fe was used as a threshold to separate between oxic and anoxic soil  
161 solution samples.

162

## 163 2.2. *Sample preparation and analysis*

164 Approximately, 0.25-0.40 g of soil samples were digested in a mixture of concentrated  
165  $\text{HNO}_3$ , HF and  $\text{H}_2\text{O}_2$  (ratio 3:2:1) in PFA beakers (Savillex<sup>®</sup> MN, USA) for 24-36 h on a hotplate  
166 at  $120^\circ\text{C}$ . The digests were evaporated until dryness on a hot plate at  $70^\circ\text{C}$ . To remove excess HF,  
167 the dried residues were redigested with a mixture of concentrated HCl and  $\text{HNO}_3$  for at least 3-4  
168 hours, refluxed several times and evaporated to dryness on a hot plate. Samples were finally  
169 dissolved in  $7 \text{ mol L}^{-1}$  HCl and 0.001%  $\text{H}_2\text{O}_2$ . The water samples (approximately 300 mL) were  
170 evaporated yielding  $>300 \text{ ng}$  of Cu for isotope analysis. The samples were refluxed in  $\text{HNO}_3$  and  
171  $\text{H}_2\text{O}_2$  (ratio 1:1) and finally dissolved in  $7 \text{ mol L}^{-1}$  HCl and 0.001%  $\text{H}_2\text{O}_2$  for Cu purification.

172 All samples were purified using Poly-Prep Chromatography columns (Bio-Rad, CA, USA)  
173 filled with 2 mL of pre-cleaned 100-200 mesh AG MP-1 (Bio-Rad, CA, USA) anion exchange  
174 resin following an established method (Bigalke et al., 2010a). For soil samples, the column  
175 purification was repeated once to gain matrix-clean Cu fractions (Bigalke et al., 2011; Petit et al.,  
176 2012). After complete separation, the purified fractions were evaporated to dryness and digested  
177 with concentrated  $\text{HNO}_3$  and  $\text{H}_2\text{O}_2$ . The samples were evaporated and then dissolved in 2%  $\text{HNO}_3$   
178 for Cu isotope analysis. All samples were analyzed by ICP-MS (7700x, Agilent, CA, USA) for  
179 matrix elements and Cu recovery. Column eluates, in which Cu was not completely recovered  
180 ( $100\pm 6\%$ ) or in which matrix elements were present, were discarded and sample purification was  
181 repeated.

182 All reagents used were of suprapur quality (Merck, Darmstadt, Germany). Hydrochloric  
183 and nitric acid were purified by sub-boiling distillation. Sample preparation and chemical



184 purification were performed in the clean chemistry laboratory at the Institute of Geology,  
185 University of Bern. Total procedural Cu blanks averaged  $1.9 \pm 0.9$  ng ( $n=3$ ) and  $3.4 \pm 1.5$  ng ( $n=3$ )  
186 for the first and second runs of column purification, respectively. The quality of the method was  
187 evaluated by using USGS basalt BCR-2 (Basalt Columbia River 2, USGS, Reston, VA, USA)  
188 reference materials. The mean total Cu concentration we determined in BCR-2 was  $18.6 \pm 0.3$   $\mu\text{g}$   
189  $\text{g}^{-1}$  (mean  $\pm$  SD,  $n=11$ ) in good agreement with the certified value of  $19 \pm 2$   $\mu\text{g}$   $\text{g}^{-1}$ .

190

### 191 **2.3. Isotope analysis**

192 Copper isotope ratios were analyzed by MC-ICP-MS (Thermo-Finnigan Neptune, Thermo  
193 Scientific, Waltham, MA, USA) at the Leibniz University Hannover, Germany. Instrument was  
194 operating in the low mass resolution mode. Samples and standards were diluted to  $300$   $\mu\text{g}$   $\text{L}^{-1}$  Cu  
195 with 2%  $\text{HNO}_3$  and introduced in to the MC-ICP-MS by a glass spray chamber (double pass Scott  
196 design). Nickel (NIST 986, National Institute of Standards and Technology, Gaithersburg, MD,  
197 USA) at concentration of  $1000$   $\mu\text{g}$   $\text{L}^{-1}$  was used for the instrumental mass-bias correction in  
198 combination with standard-sample bracketing. Every sample was at least analyzed twice. The  
199 average Cu isotope ratio was reported in the  $\delta^{65}\text{Cu}$  notation in ‰ relative to NIST 976. The  
200 accuracy of the resin purification method was validated by using spiked Cu-free matrix samples.  
201 The Cu-free matrix samples were prepared from the matrix fraction derived from the purification  
202 of the original samples and spiked with the  $\text{ERM}^{\text{®}}$ -AE633 Cu isotope standards (Institute for  
203 Reference Materials and Measurements, Geel, Belgium), which is isotopically identical with NIST  
204 976 (Moeller et al., 2012). The spiked matrices were treated and purified in the same manner as  
205 the original samples. The  $\delta^{65}\text{Cu}$  value of the matrix samples was  $-0.03 \pm 0.04$ ‰ (mean  $\pm$  2SD,  $n=5$ )  
206 and undistinguishable from  $\text{ERM}^{\text{®}}$ -AE633 ( $-0.01 \pm 0.05$ ‰, Moeller et al., 2012). Reproducibility

207 and accuracy of  $\delta^{65}\text{Cu}$  measurements were monitored with the help of certified reference materials  
 208 BCR-2 and NBS C 125-2 (SRM C1252, National Institute of Standards and Technology,  
 209 Gaithersburg, MD, USA). The NBS C 125-2 was used as an in-house Cu standard to check the  
 210 MC-ICP-MS stability yielding a  $\delta^{65}\text{Cu}$  value of  $0.36\pm 0.06\%$  (mean $\pm$ 2SD, n=10). BCR-2 yielded  
 211 a  $\delta^{65}\text{Cu}_{\text{NIST976}} = 0.15\pm 0.08\%$  (mean $\pm$ 2SD, n=11) comparable to the previously published data  
 212 ranging from  $0.14\pm 0.05\%$  to  $0.22\pm 0.06\%$  (e.g., Bigalke et al., 2010a; 2013; Liu et al., 2014b;  
 213 Moeller et al., 2012).

214

#### 215 **2.4. Calculations and statistics**

216 The overall mass flux for any soil volume  $m_{j;\text{flux}}$  in  $\text{g cm}^{-2}$  was then calculated for each element j  
 217 using Eq. (1) proposed by Brimhall et al. (1991) and modified by Egli and Fitze (2000):

$$218 \quad m_{j;\text{flux}} = \frac{1}{100} \times \frac{\rho_{\text{ref}} \times C_{j;\text{ref}} \times Th \times \tau_{j;\text{w}}}{\varepsilon_{i;\text{w}} + 1} \quad (1)$$

219 in which  $\rho$  is the bulk density,  $C_j$  is the concentration of j in weight percent,  $Th$  (cm) is the  
 220 thickness of the considered soil horizon. The subscripts ref and w refer to the soil taken as a  
 221 reference and to the weathered product, respectively. We used positions 60 and 110 m as  
 222 representing the weathered product (because drainage changes the soil composition at these  
 223 distances) and positions 210 and 400 m as reference (because here the effect of drainage is very  
 224 low, Montagne et al., 2008). This is different to the classical approach of comparing soil horizons  
 225 with parent material. The  $\varepsilon_{i;\text{w}}$  and  $\tau_{j;\text{w}}$  values are the strain and the open-system mass-transport  
 226 functions, respectively, calculated according to Eqs. 2 and 3 (Brimhall et al., 1991). The  $\varepsilon_{i;\text{w}}$  is a  
 227 measure for the change of the soil volume over time using an immobile element i and  $\tau_{j;\text{w}}$  is the  
 228 mass fraction of element j gained or lost from the weathered product with respect to the mass

229 originally present in the reference material (i.e. the soil at positions 210 and 400 m). We used  
 230 quartz as an immobile compound.

$$231 \quad \varepsilon_{i;w} = \frac{\rho_{ref}C_{i;ref}}{\rho_w C_{i;w}} - 1 \quad (2)$$

$$232 \quad \tau_{i;j} = \frac{\rho_w C_{i;j}}{\rho_{ref}C_{j;ref}} (\varepsilon_{i;w} + 1) - 1 \quad (3)$$

233 After checking the data for homoscedasticity with the Levené test, an analysis of variance  
 234 (ANOVA) followed by a Tukey's Honestly Significant Difference (HSD) post hoc test was  
 235 conducted to compare the mean Cu concentrations and isotopic compositions among soil volumes.  
 236 Normal distribution of residuals was checked by visual inspection. Significance was set at  $p <$   
 237 0.05.

238

### 239 3. Results

240 Copper concentrations in the bulk horizons increased with depth at three of the four  
 241 positions (1.1, 2.1 and 4.0 m). Copper concentrations were closely related with those of the clay  
 242 fraction (Fig. 3a). The Cu concentrations in the surface (Ap) horizon and clay-rich Bt horizons  
 243 varied only little along the trench. In contrast, in the E&Bt-horizon, there was a large lateral  
 244 variation in the Cu concentrations, with the lowest value at position 0.6 m (Tab. 1, Fig. 4a). The  
 245  $\delta^{65}\text{Cu}$  values tended to decrease from the Ap horizon to the deeper horizons (Fig. 4b), but showed  
 246 no relation to Cu concentrations or the clay fraction (Fig. 3b). However, the  $\delta^{65}\text{Cu}$  values at  
 247 different depths in the E&Bt and Bt horizons and at the different positions along the trench were  
 248 not different. We only detected a single much lower  $\delta^{65}\text{Cu}$  value compared to all other samples in  
 249 the 35-45 cm depth layer (E&Bt horizon) at position 0.6 m (Tab. 1, Fig. 3b, 4b).

250 The Cu concentrations were significantly higher in the black and ochre volumes than in the  
251 pale-brown and white-grey volumes, respectively. Copper concentrations were not related with  
252 distance to the drain in pale-brown and white-grey volumes but were lower in the black and ochre  
253 volumes at position 0.6 m than at all other positions (Fig. 5a, Tukeys HSD test,  $p < 0.05$ ). Overall  
254 the black volumes had the significantly highest and the ochre volumes the significantly lowest  
255  $\delta^{65}\text{Cu}$  values, while the  $\delta^{65}\text{Cu}$  values of the pale-brown and white-grey volumes were not  
256 significantly different from those of the ochre and black volumes (Fig. 6). The bulk  $\delta^{65}\text{Cu}$  value  
257 calculated from the mass-balanced sum of the individual soil volumes (ranging from  $-0.36 \pm 0.04\text{‰}$   
258 to  $-0.41 \pm 0.04\text{‰}$ ) showed good agreement with the  $\delta^{65}\text{Cu}$  value of the bulk soil in the E&Bt horizon  
259 at the different distances from the drain (ranging from  $-0.38 \pm 0.03\text{‰}$  to  $-0.41 \pm 0.02$ ). At position  
260 0.6 m, this is true for the lower bulk sample (45-55 cm depth), which overlaps with the depth where  
261 soil volumes were sampled (Fig. 2), while for the upper 35-45 cm depth layer of the E&Bt horizon  
262 with the low  $\delta^{65}\text{Cu}$  value ( $-0.91 \pm 0.15\text{‰}$ ) we did not have samples of individual soil volumes for  
263 comparison.

264 The dissolved Cu concentrations in the porous cup sample were highest of all analyzed soil  
265 solutions. The Cu concentrations of drain water were consistently lower than those of the  
266 piezometer sample in all three studied samples (Tab. 2). While in the hydrological year 2005/2006  
267 the  $\delta^{65}\text{Cu}$  values in the piezometer and drain waters seemed to be lower in the anoxic samples ( $\text{Fe}$   
268  $> 40 \mu\text{g L}^{-1}$ ); compared to the oxic samples, the  $\delta^{65}\text{Cu}$  values of the anoxic samples were similar  
269 to those in the oxic samples from the Piezometer in the following hydrological year 2007/08.  
270 Consequently, the variations in  $\delta^{65}\text{Cu}$  values among the various solution types and sampling dates  
271 could neither be clearly assigned to redox conditions nor to the way of sampling. There was no  
272 clear difference in Cu concentrations in waters taken under anoxic conditions ( $\text{Fe} > 40 \mu\text{g L}^{-1}$ )

273 compared with oxic conditions ( $\text{Fe} < 40\mu\text{g L}^{-1}$ ). There were no clear differences in  $\delta^{65}\text{Cu}$  values  
274 among the water samples from the piezometers and the drain in 2005/2006, but small variations in  
275 2007/08. The single porous cup sample showed the lowest  $\delta^{65}\text{Cu}$  value. Overall, the water samples  
276 showed higher  $\delta^{65}\text{Cu}$  values than the solid soil samples, with  $\Delta^{65}\text{Cu}_{(\text{soil-solution})} = -0.61 \pm 0.41$ .

277

## 278 4. Discussion

### 279 4.1. *Depth distribution of Cu concentrations and $\delta^{65}\text{Cu}$ values*

280 The vertical distribution of Cu in the study soil is influenced by (1) the amendment of limed sludge  
281 from 1998 to 2001 resulting in a Cu input of approx.  $0.9 \text{ g m}^{-2}$  (Montagne et al., 2007), (2) regular  
282 fertilization e.g., with mineral fertilizer (no manure application) and (3) pedogenetic processes  
283 including lessivation and hydromorphy (Montagne et al., 2008). The Cu input with sludge and  
284 fertilizer has increased Cu concentrations in the Ap horizons and also might have changed the  
285  $\delta^{65}\text{Cu}$  value. In the deeper horizons, clay eluviated from the Ap horizons which accumulated in  
286 the Bt horizons likely explains the increase in Cu concentrations because the clay fraction usually  
287 contains higher Cu concentrations than the coarser particle sizes (Minkina et al., 2011). The latter  
288 is also confirmed by the close correlation between the clay and the Cu concentrations ( $r = 0.80$ ;  $p$   
289  $< 0.001$ ). This correlation even became closer, when Ap horizons (with anthropogenic Cu input)  
290 were removed (Fig. 3a). No  $\delta^{65}\text{Cu}$  values for agriculturally used sludge or mineral fertilizers have  
291 up to now been reported. However, in case that these additions carry a heavier  $\delta^{65}\text{Cu}$  value than  
292 the soil they might be responsible for the higher  $\delta^{65}\text{Cu}$  values in the Ap horizons. The different soil  
293 depths in E&Bt and Bt horizons show no significant  $\delta^{65}\text{Cu}$  changes, despite the significant changes  
294 in Cu concentrations linked to the clay eluviation. We explain this finding by the fact that Cu  
295 bound to clay controls the concentration and the  $\delta^{65}\text{Cu}$  value of total soil Cu. Our findings suggests

296 that lessivage does not change  $\delta^{65}\text{Cu}$  values of the bulk soils, because the eluviated and illuviated  
297 horizons have the same Cu isotopic composition. The lacking influence of clay concentrations on  
298  $\delta^{65}\text{Cu}$  values is reflected by the absence of a correlation between these two variables ( $r < 0.001$ ,  $p$   
299  $= 0.95$ ). Furthermore, soil volumes with different clay concentrations (Montagne et al, 2008) did  
300 not show a significant difference in  $\delta^{65}\text{Cu}$  values, again indicating that other soil processes than  
301 the clay concentration (e.g. sludge application, weathering; Fig. 7) controlled Cu isotope ratios.

302

#### 303 **4.2. Response of Cu concentrations and $\delta^{65}\text{Cu}$ values to drainage**

304 The low Cu concentration in the E&Bt at position 0.6 m, suggests that the drainage induced Cu  
305 leaching (Table 1, Fig. 4a). Mass flux calculations indicated that Cu mass flux ( $m_{\text{Cu flux}}$ ) at position  
306 0.6 m was, on average, three times higher than at positions 2.1 and 4.0 m (43.8 and 15.3  $\text{mg cm}^{-2}$ ,  
307 respectively). This loss of Cu from the E&Bt horizon at position 0.6 m is linked with substantial  
308 loss of Fe and clay at positions 0.6 m and 1.1 m, (6.5 and 2.3  $\text{kg m}^{-2}$  Fe and 75.8 and 25.6  $\text{kg m}^{-2}$   
309 clay, respectively; Montagne and Cornu, 2010). The loss has been explained by strongly enhanced  
310 eluviation caused by drainage-induced higher water fluxes, and is most pronounced in the upper  
311 part of the E&Bt horizon at position 0.6 m (Montagne and Cornu, 2010). These findings agree  
312 with the close correlation between the clay and the Cu concentrations (Fig. 3a), which furthermore  
313 suggests that clay is the dominant Cu pool in this soil. In contrast, the observed eluviation had no  
314 significant effect on the  $\delta^{65}\text{Cu}$  value of the drained soil, as illustrated by the lack of a correlation  
315 between  $\delta^{65}\text{Cu}$  values and clay concentrations (Fig. 3b).

316 At 0.6 m distance, the E&Bt horizon showed a strong negative  $\delta^{65}\text{Cu}$  value in its upper part  
317 (35-45cm), while its lower part (45-55cm) with similar properties (clay and Cu concentrations)  
318 did not show differences in  $\delta^{65}\text{Cu}$  values from the soil at other distances (Fig. 3b). This strongly

319 negative value was ascertained by three replicate analyses including separate digestion,  
320 purification and analysis of each replicate. We suggest that the light  $\delta^{65}\text{Cu}$  value in the upper part  
321 of the E&Bt horizon at position 0.6 m might be attributable to the change in redox conditions  
322 following drainage. Redox changes can cause a comparatively large fractionation of  $\delta^{65}\text{Cu}$  values  
323 with the reduced Cu(I) enriched in the light isotopes (Fig. 1; Zhu et al., 2002). Under anoxic  
324 conditions, the reduced Cu fraction may account for a major part of total soil Cu and may carry a  
325 heavy isotope signal to balance that of a Cu-isotopically light residual fraction (Kusonwiriya Wong  
326 et al., 2015). This Cu-isotopically heavy reduced fraction might be lost by oxidation (Fulda et al.,  
327 2013b) attributable to drainage, leaving the residual Cu isotopically lighter. The reason for the  
328 absence of this isotope effect in the deeper E&Bt Horizon (45-55cm), might be its closer proximity  
329 to the soil water table and thus less pronounced episodic oxidation. Fekiacova et al. (2015) reported  
330 a similar negative value (-0.89 ‰) for a Retisol at approximately the same depth, which they  
331 interpreted as light Cu enrichment linked to Fe oxide precipitation and sorption of light Cu leached  
332 from the surface horizons. However, Fekiacova et al. (2015) observed an increase in Cu  
333 concentrations in contrast to our study soil where the low  $\delta^{65}\text{Cu}$  value was related with a decrease  
334 in Cu concentrations. Consequently, the low  $\delta^{65}\text{Cu}$  values in the study of Fekiacova et al. (2015)  
335 and ours must have different reasons.

336         Additionally to analyzing the bulk soil samples, we partitioned the soil in the E&Bt horizon  
337 into four different soil volumes. The differentiation starts from the ochre volume, developing  
338 successive pale-brown and white-grey soil volumes by increasing eluviation and redox-induced  
339 bleaching (Montagne et al., 2008). Within the ochre volume, the black volume forms because of  
340 the precipitation of Mn oxides. With increasing proximity to the drain the ochre volumes decreased  
341 and the black, pale-brown and white-grey volumes increased (Montagne et al., 2008). The black

342 volumes always had the highest Cu concentrations, probably because of precipitation with and  
343 sorption of Cu on Mn oxides (Negra et al., 2005). The ochre volume always showed higher Cu  
344 concentrations than the pale-brown and white grey volumes because of eluviation and reductive  
345 leaching of clay minerals and (oxyhydr)oxides in the latter two volumes (Fig. 5a, Montagne et al.,  
346 2008). Because of the drainage, Cu concentrations in the black and ochre volumes decreased by  
347 approx. 50% in the direct vicinity (position 0.6 m) of the drain, which is consistent with the  
348 decrease in the bulk soil. The decrease in the Cu concentrations of the ochre and black volumes at  
349 position 0.6 m is driven by the strong clay loss by eluviation. In contrast, the more oxidizing  
350 conditions near the drain caused an increase in the abundance of the ochre and black volumes,  
351 attributable to the precipitation of Mn and Fe oxi(hydr)oxides. Because ochre and black volumes  
352 formed in a soil, which was already depleted in Cu, they showed lower Cu concentrations..  
353 Independent of the distance to the drain, the contributions of the Cu stocks in the black, pale-brown  
354 and white-grey volumes to the total Cu stock of the bulk E&Bt horizon did not change, while the  
355 contribution of the Cu stock in the ochre volume to the total Cu stock of the bulk horizon decreased  
356 (Fig. 5b).

357         There were no clear variations in the  $\delta^{65}\text{Cu}$  values of the individual volumes with distance  
358 to the drain ( $p < 0.05$ ) indicating that the drainage-induced morphological changes at position 0.6  
359 m did not cause a Cu isotope fractionation among the soil volumes. At position 0.6 m, the soil  
360 volumes were taken from the lower depth layer (45-55 cm), which had a similar  $\delta^{65}\text{Cu}$  value as all  
361 other bulk soil samples (Fig. 2). The black volumes showed always significantly higher  $\delta^{65}\text{Cu}$   
362 values than the ochre volumes they develop from. This might be attributable to variable redox at  
363 the small spatial scale at which the differentiation into the four soil volumes occurred and related  
364 Cu isotope fractionation or by the sorption on Fe and Mn oxy(hydr)oxides in the black volumes.



365 As redox variation usually causes a strong isotope fractionation (Fig. 1) we consider more likely  
366 that the limited changes observed in the  $\delta^{65}\text{Cu}$  values of the different soil volumes depended on  
367 the adsorption to Fe and Mn (oxyhydr)oxides (which preferentially adsorb heavy isotopes, Fig. 1b,  
368 Pokrovsky et al., 2008; Balistrieri et al., 2008).

369 The overall lack of a correlation between the clay concentration and  $\delta^{65}\text{Cu}$  values, the  
370 differences in  $\delta^{65}\text{Cu}$  values between the 35-45 and 45-55cm depth layers despite a similar degree  
371 of eluviation and the absence of significant variations between the ochre and the white-grey soil  
372 volumes (Fig. 5, the white grey volume is clay-depleted) imply limited importance of clay  
373 eluviation for the  $\delta^{65}\text{Cu}$  values of the soil, despite the marked effect of lessivation on Cu  
374 concentrations in bulk horizons (Fig. 3).

375

#### 376 **4.3. *Cu in soil water***

377 The Cu concentrations in our soil water samples were similar to the previously published  
378 range of Cu concentrations in soil pore water during weathering of black shale of 1-16  $\mu\text{g L}^{-1}$   
379 (Mathur et al., 2012), dissolved Cu in river of 0-3  $\mu\text{g L}^{-1}$  (Vance et al., 2008) and dissolved Cu in  
380 wetlands 1-12  $\mu\text{g L}^{-1}$  (Babcsányi et al., 2014). The low concentrations in the drain water may be  
381 caused by co-precipitation with or sorption to Mn and/or Fe (oxyhydr)oxides precipitating near  
382 the drain pipe where the reduced Mn and Fe comes into contact with oxygen. Samples with low  
383 (<40  $\mu\text{g L}^{-1}$ ) and high (>40  $\mu\text{g L}^{-1}$ ) Fe concentrations (indicative for oxic and reducing conditions,  
384 respectively) did not show systematically different Cu concentrations, indicating that the redox  
385 potential was not sufficiently low to reduce Cu.

386 The  $\delta^{65}\text{Cu}$  values in our water samples are well within the range reported for soil, river,  
387 and wetland water ranging from 0.02-1.45‰ (Vance et al., 2008; Mathur et al., 2012; Babcsányi

388 et al., 2014). The  $\delta^{65}\text{Cu}$  values during anoxic conditions in 2005/06 overlapped with those during  
389 oxic conditions in 2007/08, showing no clear relationship with the redox potential in the  
390 piezometer. In the drain water, the  $\delta^{65}\text{Cu}$  values seemed to be lower under anoxic conditions, but  
391 were similar to the oxic sample from the piezometer in 2007/08. The uniform Cu concentrations  
392 and  $\delta^{65}\text{Cu}$  values indicate that there was no redox-induced change in Cu mobility, agreeing well  
393 with the findings from the bulk soils, where we also did not observe an indication for redox  
394 mobilization of Cu. The  $\delta^{65}\text{Cu}$  value of dissolved Cu was heavier than that of the bulk solid soil  
395 ( $\Delta^{65}\text{Cu}_{(\text{soil-solution})} = -0.61 \pm 0.41$ ), but fractionation was less pronounced than reported for redox-  
396 induced fractionations in field and laboratory experiments (Fig. 1). The pattern of Cu isotopically  
397 light solid soils and heavy dissolved Cu fits well into the findings of a weathering experiments  
398 with basalts at pH 5 (Li et al. 2016) and results of the analysis of soil solutions from oxic  
399 weathering of black shales, which both always showed an enrichment of the isotopically heavy  
400 Cu in the dissolved phase (Mathur et al., 2012).

401           Independent of the redox conditions, the  $\delta^{65}\text{Cu}$  values of the dissolved fraction in rivers,  
402 wetlands and soils always showed a heavy  $\delta^{65}\text{Cu}$  value, while the particulate and colloidal fraction  
403 showed light  $\delta^{65}\text{Cu}$  values and a strong response to redox changes (Babcsányi et al, 2014; Vance  
404 et al., 2008). The lack of a relationship of the  $\delta^{65}\text{Cu}$  values of dissolved Cu with the redox potential  
405 might be explained by the fact that the Cu isotope ratio of dissolved Cu in soils and rivers is more  
406 strongly controlled by complexation with strong dissolved ligands (Vance et al., 2008, Vance et  
407 al., 2016) than by redox changes. The responsible ligands were identified by cathode-stripping  
408 voltametry and are subdivided in the ligand classes L1 and L2 (Muller et al., 2001). Both ligand  
409 classes have high stability constants up to  $10^{16}$  and often occur in excess compared to Cu

410 concentrations in solution (Vance et al., 2008). Therefore, it can be assumed that almost all  
411 dissolved Cu occurs in complexed form in environmental solutions (Muller et al., 2001).

412

## 413 **5. Conclusions**

414 1) The slightly decreasing  $\delta^{65}\text{Cu}$  values with increasing depth in the bulk soils might be  
415 caused by addition of heavy Cu (e.g., fertilizer and sewage sludge) to the surface soil.

416 2) Drainage did not change  $\delta^{65}\text{Cu}$  values in bulk soil and soil volumes, despite Cu  
417 redistribution by enhanced clay eluviation, with the exception of one point. A low  
418  $\delta^{65}\text{Cu}$  value and Cu concentration in the upper E&Bt horizon near to the drain may  
419 indicate oxidative weathering and leaching of heavy Cu isotopes formerly stored in the  
420 reduced Cu pool and is the only  $\delta^{65}\text{Cu}$  value which we could link to redox changes.

421 The drainage caused changes in the Cu distribution among the soil volumes indicative  
422 of locally changed pedogenetic processes. The  $\delta^{65}\text{Cu}$  values showed significant  
423 differences among the soil volumes but did not change with distance to the drain,  
424 indicating that the Cu isotope signals are dominated by sorption processes but little by  
425 redox changes.

426 3) The Cu concentrations and  $\delta^{65}\text{Cu}$  values in the solution samples did not respond to  
427 changes in soil redox conditions, indicating that short-term changes in redox conditions  
428 in the soil have a small or no effect on the isotope signals of dissolved Cu. The overall  
429  $\delta^{65}\text{Cu}$  value of dissolved Cu was heavier than that of bulk solid soil ( $\Delta^{65}\text{Cu}_{(\text{soil-solution})} =$   
430  $-0.61 \pm 0.41$ ), which we attribute to weathering and sorption of dissolved Cu to strong  
431 ligands in solution in line with several reports of soils solutions and river waters in the  
432 literature.

433

434 A conceptual model of the effect of the different processes on Cu distribution and  $\delta^{65}\text{Cu}$   
435 values in the soil is displayed in Fig. 7. In summary, the two dominant pedogenetic processes in  
436 the study soils (lessivation and hydromorphy) seem to have limited influence on the Cu stable  
437 isotope ratios although lessivation strongly controls Cu concentrations. The effect of drainage on  
438  $\delta^{65}\text{Cu}$  is visible only at one position close to the drain, which probably showed the strongest change  
439 in redox conditions. Our results illustrate that redox induced Cu leaching is only visible where the  
440 soil is most oxidized. Instead, in the Retisol clay eluviation and leaching of organically complexed  
441 Cu, drive Cu mobility. In general the  $\delta^{65}\text{Cu}$  approach on bulk soils is helpful to investigate the  
442 influence of redox and sorption processes on Cu mobility in the soil system, but does not help for  
443 clay eluviation were two pools (e.g. clay and soil) are isotopically not discernible. The application  
444 of  $\delta^{65}\text{Cu}$  values to investigate into redox controlled Cu mobility might be of high importance as  
445 reductive Cu mobilisation is driving the mobilisation of a number highly relevant pollutant  
446 elements (Ag, Cd, Hg, Pb; Abgottspon et al., 2015; Hofacker et al., 2013b; Weber et al., 2009b).

447

#### 448 **Acknowledgments**

449 We thank the group of Isotope Geology of the University of Berne, Klaus Mezger, Thomas Nägler,  
450 Igor Villa and Gabriela Balzer for access to the clean room and support. The authors are grateful  
451 to L. Prud'Homme, B. Renault, G. Giot, N. Chigot from URSol (INRA, Orléans, France) for field  
452 sampling and monitoring. We thank the AE Edward Nater, and Ryan Mathur as well as two  
453 anonymous reviewers for their constructive comments, which significantly improved the  
454 manuscript. We thank the Agricultural Research Development Agency (Public Organization),  
455 ARDA, Thailand, for funding Charirat Kusonwiriawong.

456

457 **References**

- 458 Abgottspon, F., Bigalke, M., Wilcke, W., 2015. Fast colloidal and dissolved release of trace  
459 elements in a carbonatic soil after experimental flooding. *Geoderma* 259-260, 156-163.
- 460 Babcsányi, I., Imfeld, G., Granet, M., Chabaux, F. 2014., Copper stable isotopes to trace copper  
461 behavior in wetland systems. *Environ. Sci. Technol.* 48, 5520-5529.
- 462 Balint, R., Nechifor, G., Ajmone-Marsan, F., 2014. Leaching potential of metallic elements from  
463 contaminated soil under anoxia. *Environ. Sci. Process Impacts* 16, 211-219.
- 464 Balistrieri, L.S., Borrok, D.M., Wanty, R.B., Ridley, W.I., 2008. Fractionation of Cu and Zn  
465 isotopes during adsorption onto amorphous Fe(III) oxyhydroxide: experimental mixing of  
466 acid rock drainage and ambient river water. *Geochim. Cosmochim. Acta* 72, 311–328.
- 467 Bigalke, M., Weyer, S., Wilcke, W., 2010a. Stable copper isotopes: A novel tool to trace copper  
468 behavior in hydromorphic soils. *Soil Sci. Soc. Am. J.* 74, 60-73.
- 469 Bigalke, M., Weyer, S., Wilcke, W., 2010b. Copper isotope fractionation during complexation  
470 with insolubilized humic acid. *Environ. Sci. Technol.* 44, 5496–5502.
- 471 Bigalke, M., Weyer, S., Kobza, J., Wilcke, W., 2010c. Stable Cu and Zn isotope ratios as tracers  
472 of sources and transport of Cu and Zn in contaminated soil. *Geochim. Cosmochim. Acta*  
473 74, 6801–6813.
- 474 Bigalke, M., Weyer, S., Wilcke, W. 2011., Stable Cu isotope fractionation in soils during oxic  
475 weathering and podsolization. *Geochim. Cosmochim. Acta* 75, 3119–3134.

- 476 Bigalke, M., Kersten M., Weyer, S., Wilcke, W. 2013., Isotopes trace biogeochemistry and  
477 sources of Cu and Zn in an intertidal soil. . Soil Sci. Soc. Am. J. 77, 680-691.
- 478 Borch, T., Kretzschmar, R., Kappler, A., Van Cappellen, P., Ginder-Vogel, M., Voegelin, A.,  
479 Campbell, K., 2010. Biogeochemical redox processes and their impact on contaminant  
480 dynamics. Environ. Sci. Technol. 44, 15-23.
- 481 Brimhall, G.H., Chadwick, O.A., Lewis, C.J., Compston, W., Williams, I.S., Danti, K.J.,  
482 Dietrich, W.E., Power, M.E., Hendricks, D., Bratt, J., 1992. Deformational mass-  
483 transport and invasive processes in soil evolution. Science 255, 695-702.
- 484 Clayton, R.E., Hudson-Edwards, K.A., Houghton, S.L., 2005. Isotopic effects during Cu sorption  
485 onto goethite. Geochim. Cosmochim. Acta, 69(10) , A216-a216.
- 486 Cornu, S., Montagne, D., Daroussin, J., Cousin, I., 2012. Image-analytically derived conceptual  
487 model of Albeluvisol morphological degradation induced by artificial drainage in France.  
488 Geoderma 189-190, 296-303.
- 489 Du Laing, G., Rinklebe, J., Vandecasteele, B., Meers, E., Tack, F. M. G., 2009. Trace metal  
490 behaviour in estuarine and riverine floodplain soils and sediments: A review. Sci.Total  
491 Environ. 407, 3972-3985.
- 492 Egli, M. and Fitze, P. (2000) Formulation of pedologic mass balance based on immobile  
493 elements: A revision. Soil Sci. 165, 437-443.
- 494 Ehrlich, S., Butler, I., Halicz, L., Rickard, D., Oldroyd, A., Matthews, A., 2004. Experimental  
495 study of the copper isotope fractionation between aqueous Cu(II) and covellite, CuS.  
496 Chem. Geol. 209,259-269.

- 497 FAO., 2001. Lecture notes on the major soils of the world. In World Soil Resources Report No.  
498 94. Driessen, P., Deckers J., Spaargaren, O., and Nachtergaele, F., Eds., Rome.
- 499 Fekiacova, Z., Cornu, S., Pichat, S., 2015. Tracing contamination sources in soils with Cu and  
500 Zn isotope ratios. *Sci. Total Environ.* 517, 96-105.
- 501 Fulda, B., Voegelin, A., Maurer, F., Christl, I., Kretzschmar, R., 2013a. Copper redox  
502 transformation and complexation by reduced and oxidized soil humic acid. 1. X-ray  
503 absorption spectroscopy study. *Environ. Sci. Technol.* 47, 10903-10911.
- 504 Fulda, B., Voegelin, A., Ehlert, K., Kretzschmar, R., 2013b. Redox transformation, solid phase  
505 speciation and solution dynamics of copper during soil reduction and reoxidation as  
506 affected by sulfate availability, *Geochim. Cosmochim. Acta* 123, 385-402.
- 507 Hofacker, A.F., Voegelin, A., Kaegi, R., Weber F.-A., Kretzschmar, R., 2013a. Temperature-  
508 dependent formation of metallic copper and metal sulfide nanoparticles during flooding  
509 of a contaminated soil. *Geochim. Cosmochim. Acta* 103, 316-322.
- 510 Hofacker, A.F., Voegelin, A., Kaegi, R., Kretzschmar, R., 2013b. Mercury Mobilization in a  
511 Flooded Soil by Incorporation into Metallic Copper and Metal Sulfide Nanoparticles.  
512 *Environmental Science & Technology*, 47(14): 7739-7746.
- 513 Ilina, S.M., Viers, J., Lapitsky, S.A., Mialle, S., Mavromatis, V., Chmeleff, J., Brunet, P.,  
514 Alekhin, Y.V., Isnard, H., Pokrovsky, O.S., 2013. Stable (Cu, Mg) and radiogenic (Sr,  
515 Nd) isotope fractionation in colloids of boreal organic-rich waters. *Chem. Geol.* 342: 63-  
516 75.

- 517 IUSS Working Group WRB. 2014. World Reference Base for Soil Resources 2014. International  
518 soil classification system for naming soils and creating legends for soil maps. World Soil  
519 Resources Reports No. 106. FAOM Rome.
- 520 Jouvin, D., Weiss, D.J., Mason, T.F.M., Bravin, M.N., Louvat, P., Zhao, F., Ferec, F.,  
521 Hinsinger, P., Benedetti, M.F., 2012. Stable isotope of Cu and Zn in higher plants:  
522 Evidence for Cu reduction at the root surface and two conceptual models for isotopic  
523 fractionation processes. *Environ. Sci. Technol.* 46, 2652-2660.
- 524 Kusonwiriawong, C., Bigalke, M., Abgottspon, F., Lazarov, M., Wilcke, W., (2016) Response  
525 of Cu partitioning to flooding: A  $\delta^{65}\text{Cu}$  approach in a carbonatic alluvial soil. *Chemical*  
526 *Geology* 420, 69-76.
- 527 Li, D., Liu, S.-A., Li, S., 2015. Copper isotope fractionation during adsorption onto kaolinite:  
528 Experimental approach and applications. *Chem. Geol.* 396, 74-82.
- 529 Li, D., Liu, S.-A., Li, S., 2016. Copper isotope fractionation during basalt weathering at pH =  
530 0.3, 2, 5 and T = 25°C. *Goldschmidt Abstracts*: 1743.
- 531 Liu, S.-A., Teng, F.-Z., Li, S., Wei, G.-J., Ma, J.-L., Li, D., 2014a. Copper and iron isotope  
532 fractionation during weathering and pedogenesis: Insights from saprolite profiles.  
533 *Geochim. Cosmochim. Acta* 146, 59-75.
- 534 Liu, S.-A., Li, D., Li, S., Teng, F.-Z., Ke, S., He, Y., Lu, Y., 2014b. High-Precision copper and  
535 iron isotope analysis of igneous rock standards by MC-ICP-MS. *J. Anal. At. Spectrom.*  
536 29, 122-133.



- 537 Mathur, R., Fantle, M.S., 2015. Copper Isotopic Perspectives on Supergene Processes:  
538 Implications for the Global Cu Cycle. *Elements*, 11(5): 323-329.
- 539 Mathur, R., Jin, L., Prush, V., Paul, J., Ebersole, C., Fornadel, A., Williams, J.Z., Brantley, S.,  
540 2012. Cu isotopes and concentrations during weathering of black shale of the Marcellus  
541 Formation, Huntingdon County, Pennsylvania (USA). *Chem. Geol.* 304, 175-184.
- 542 Mathur, R., Ruiz, J., Titley, S., Liermann, L., Buss, H., Brantley, S., 2005. Cu isotopic  
543 fractionation in the supergene environment with and without bacteria. *Geochim.*  
544 *Cosmochim. Acta*, 69(22): 5233-5246.
- 545 Minkina, T.M., Pinskii, D.L., Mandzhieva, S.S., Antonenko, E.M., Sushkova, S.N., 2011. Effect  
546 of the particle-size distribution on the adsorption of Copper, Lead and Zinc by  
547 Chernozemic soil of Rostov Oblast. *Eurasian Soil Sci.* 44, 1193-1200.
- 548 Moeller, K., Schoenberg, R., Pedersen R.B., Weiss, D., Dong S., 2012. Calibration of the new  
549 certified reference materials ERM-AE633 and ERM-AE647 for copper and IRMM-3702  
550 for zinc isotope amount ratio determinations. *Geostand. Geoanal. Res.* 36, 177-199.
- 551 Montagne, D., Cornu, S., Bourennane, H., Baize, D., Ratié, C., King D., 2007. Effect of  
552 agricultural practices on trace-element distribution in soil. *Commun. Soil Sci. Plan.* 38,  
553 473-491.
- 554 Montagne, D., Cornu, S., Forestier, L.L., Hardy, M., Josière, O., Caner, L., Cousin, I., 2008.  
555 Impact of drainage on soil-forming mechanisms in a French Albeluvisol: Input of  
556 mineralogical data in mass-balance modeling. *Geoderma* 145, 426-438.

- 557 Montagne, D., Cornu, S., 2010. Do we need to include soil evolution module in models for  
558 prediction of future climate change. *Climatic Change* 98, 75-86.
- 559 Muller, F.L.L., Gulin, S.B., Kalvoy, A., 2001. Chemical speciation of copper and zinc in surface  
560 waters of the western Black Sea. *Mar. Chem.*, 76(4): 233-251.
- 561 Navarrete, J.U, Viveros, M., Ellzey, J.T., Borrok, D.M., 2011. Copper isotope fractionation by  
562 desert shrubs. *Appl. Geochem.* 26, 5319-5321.
- 563 Negra, C., Ross, D.S., Lanzirotti, A., 2005. Soil manganese oxides and trace metals: Competitive  
564 sorption and microfocused synchrotron X-ray fluorescence mapping. *Soil Sci. Soc. Am.*  
565 J. 69, 353-361.
- 566 Petit, J.C.J., Taillez, A., Mattielli, N., 2012. A case study of spectral and non-spectral  
567 interferences on copper isotope measurements by multi-collector ICP-MS (Wet plasma).  
568 *Geostand. Geoanal. Res.* 37, 319-335.
- 569 Petit, J.C.J., Schafer, J., Coynel, A., Blanc, G., Deycard, V.N., Derriennic, H., Lanceleur, L.,  
570 Dutruch, L., Bossy, C., Mattielli, N., 2013. Anthropogenic sources and biogeochemical  
571 reactivity of particulate and dissolved Cu isotopes in the turbidity gradient of the Garonne  
572 River (France). *Chem. Geol.*, 359: 125-135.
- 573 Pokrovsky, O. S., Viers, J., Emnova, E. E., Kompantseva, E. I., Freydier, R., 2008. Copper  
574 isotope fractionation during its interaction with soil and aquatic microorganisms and  
575 metal oxy(hydr)oxides: Possible structural control. *Geochim. Cosmochim. Acta* 72,  
576 1742-1757.
- 577 Ponnampereuma, F. N., 1972. The chemistry of submerged soils. *Adv. Agron.* 24, 29-94.

- 578 Ryan, B.M., Kirby, J.K., Degryse, F., Harris, H., McLaughlin, M.J., Scheiderich, K., 2013.  
579 Copper speciation and isotopic fractionation in plants: uptake and translocation  
580 mechanisms. *New Phytol.* 199, 367-378.
- 581 Ryan, B.M., Kirby, J.K., Degryse, F., Scheiderich K., McLaughlin, M.J., 2014. Copper isotope  
582 fractionation during equilibration with natural and synthetic ligands. *Environ. Sci.*  
583 *Technol.* 48, 8620-8626.
- 584 Sipos, P., Nemeth, T., May, Z., Szalai, Z., 2011. Accumulation of Trace Elements in Fe-Rich  
585 Nodules in a Neutral-Slightly Alkaline Floodplain Soil. *Carpath. J. Earth Env.* 6, 13-22.
- 586 Vance, D., Archer, C., Bermin, J., Perkins, J., Staham, P.J., Lohan, M.C., Ellwood, M.J., Mills,  
587 R.A., 2008. The copper isotope geochemistry of rivers and the oceans. *Earth. Planet.Sc.*  
588 *Lett.* 274, 204-213.
- 589 Vance, D., Matthews, A., Keech, A., Archer, C., Hudson, G., Pett-Ridge, J., Chadwick, O.A.,  
590 2016. The behaviour of Cu and Zn isotopes during soil development: Controls on the  
591 dissolved load of rivers. *Chemical Geology*, 445: 36-53.
- 592 Weber, F.-A., Voegelin, A., Kretzschmar, R., 2009a. Multi-metal contaminant dynamics in  
593 temporarily flooded soil under sulfate limitation. *Environ. Sci. Technol.* 73, 5513-5527.
- 594 Weber, F.-A., Voegelin A., Kaegi, R., Kretzschmar, R., 2009b. Contaminant mobilization by  
595 metallic copper and metal sulphide colloids in flooded soil. *Nat. Geosc.* 2, 267-271.
- 596 Weinstein, C., Moynier, F., Wang, K., Paniello, R., Foriel, J., Catalano, J., Pichat, S., 2011.  
597 Isotopic fractionation of Cu in plants. *Chem. Geol.* 286, 266-271.

598 Zhu, X. K., Guo, Y., Williams, R. J. P., O'Nions, R. K., Matthews, A., Belshaw, N. S., Canters,  
599 G. W., de Waal, E. C., Weser, U., Burgess, B. K., Salvato, B., 2002. Mass fractionation  
600 processes of transition metal isotopes. *Earth. Planet. Sc. Lett.* 200, 47-62.

601 **Table 1**

602 Copper concentrations and  $\delta^{65}\text{Cu}$  values of the different soil horizons as a function of distance to  
 603 the drain.

604

Horizon	Depth (cm)	Cu ( $\mu\text{g g}^{-1}$ )	SD	$\delta^{65}\text{Cu}$ (‰)	2SD	n <sup>a</sup>
position 0.6 m						
Ap	10-20	7.3	0.1	-0.25	0.01	1
E&Bt	35-45	5.7	0.1	-0.91	0.15	3
	45-55	5.6	0.1	-0.40	0.02	1
Bt	55-65	9.1	0.2	-0.39	0.06	2
	65-75	10.8	0.4	-0.40	0.09	2
position 1.1 m						
Ap	10-20	8.1	0.6	-0.28	0.01	1
E&Bt	40-55	8.2	0.7	-0.39	0.03	1
Bt	55-65	10.7	0.2	-0.40	0.06	2
	65-80	10.5	0.3	-0.31	0.03	1
position 2.1 m						
Ap	10-20	6.5	0.1	-0.27	0.01	1
E&Bt	40-50	10.6	0.9	-0.41	0.02	2
	50-60	10.8	0.7	-0.39	0.01	2
Bt	70-83	11.4	0.3	-0.37	0.04	2
position 4.0 m						
Ap	10-20	8.5	0.2	-0.20	0.01	2
E&Bt	35-45	8.4	0.2	-0.38	0.03	1
	45-55	10.2	0.6	-0.39	0.03	1
Bt	55-65	11.7	0.8	-0.33	0.02	3
	65-75	12.0	1.1	-0.35	0.01	3

605 <sup>a</sup> n is the number of independent digestions and purifications for isotope analysis

606

607 **Table 2**

608 Copper concentration and  $\delta^{65}\text{Cu}$  values of piezometer, drain water and porous cup samples in the  
 609 hydrological years 2005/06 and 2007/08.

Sample name	2005/06						2007/08		
	Fe < 40 $\mu\text{g L}^{-1}$			Fe > 40 $\mu\text{g L}^{-1}$			Fe < 40 $\mu\text{g L}^{-1}$		
	Cu $\mu\text{g L}^{-1}$	$\delta^{65}\text{Cu}$ (‰)	2SD	Cu $\mu\text{g L}^{-1}$	$\delta^{65}\text{Cu}$ (‰)	2SD	Cu $\mu\text{g L}^{-1}$	$\delta^{65}\text{Cu}$ (‰)	2SD
Piezometer	5.5	0.40	0.08	5.3	0.10	0.09	6.5	0.11	0.03
Drain water	2.5	0.42	0.18	2.9	0.17	0.01	2.1	0.36	0.02
Porous cup	14.1	0.04	0.05						

610

611

612

613

614

615

616 **Figure captions**

617 **Fig. 1** Compilation of a)  $\delta^{65}\text{Cu}$  values found in soils, soil and river waters and b)  $\Delta^{65}\text{Cu}$  values  
 618 reported for different processes, which might be of relevance in the Retisol. <sup>1</sup>Bigalke et al.  
 619 (2011), <sup>2</sup>Bigalke et al. (2010a), <sup>3</sup>Bigalke et al. (2010c), <sup>4</sup> Vance et al. (2016), <sup>5</sup>Bigalke et al.  
 620 (2013), <sup>6</sup>Fekiacova et al. (2015), <sup>7</sup> Mathur et al. (2012), <sup>8</sup> Ilina et al. (2013), <sup>9</sup>Petit et al. (2013),  
 621 <sup>10</sup>Vance et al. (2008), <sup>11</sup>Balistrieri et al. (2008), <sup>12</sup>Clayton et al. (2005), <sup>13</sup>Pokrovsky et al. (2008),  
 622 <sup>14</sup>Li et al. (2015), <sup>15</sup>Bigalke et al. 2010b), <sup>16</sup>Ryan et al. 2014), <sup>17</sup>Ehrlich et al. (2004), <sup>18</sup>Zhu et al.  
 623 (2002), <sup>19</sup>Asael (2006), <sup>20</sup>Mathur et al. (2005), <sup>21</sup>Mathur and Fantle (2015), <sup>22</sup>Mathur et al.  
 624 (2012).

625 **Fig. 2** Schematic diagram of the study design showing the drain, the disturbed zoned caused by  
 626 subsurface drainage installation, the soil sampling depth at positions 0.6, 1.1, 2.1 and 4.0 m,  
 627 respectively, the sampling area of individual soil volumes and the sampling position of water  
 628 samples extracted from positions 0.7, 1.5 and 4.0 m, respectively and the variation of the soil water  
 629 table as registered in a piezometer.

630 **Fig. 3.** Relationship between a) the clay and Cu concentrations among all soil samples (solid line,  
 631 upper equation). If the Ap horizons (which received anthropogenic Cu) were removed, the  
 632 relationship would become stronger (dotted line, lower equation). In b), the relationship between  
 633 clay and Cu concentrations (black diamonds) and clay concentrations and  $\delta^{65}\text{Cu}$  values (open  
 634 triangles) of the E&Bt horizons are displayed separately because these horizons should initially have  
 635 a homogeneous Cu isotope signal, which is then affected by the drainage. While clay and Cu  
 636 concentrations show a strong linear correlation (solid line, equation), there was correlation between  
 637 the clay concentrations and the  $\delta^{65}\text{Cu}$  values. The red arrow illustrates the shift between the  $\delta^{65}\text{Cu}$

638 values of the uppermost sample at position 60 and the other Bt horizon samples which show identical  
639  $\delta^{65}\text{Cu}$  values.

640 **Fig. 4.** Vertical distribution of a) Cu concentrations, b)  $\delta^{65}\text{Cu}$  values of the different bulk soil  
641 horizons as a function of the distance to the drain. Horizontal bars indicate sampling depth. Vertical  
642 bars indicate a) SD of concentrations and b) 2SD of Cu isotope ratios. Vertical error bars indicate  
643 the depth interval the sample was taken from. The letters at the right site of the figure are pedogenetic  
644 horizon designations.

645 **Fig. 5.** Copper concentrations in the soil volumes at different distances from the drain (a) and Cu  
646 stock of a given soil volume (b). Horizontal error bars indicate a) SD of concentration analysis and  
647 b) error propagation based on the standard deviation of concentrations, volumes and bulk densities.

648 **Fig. 6.** Mean  $\delta^{65}\text{Cu}$  values of the four soil volumes indicative of the dominating pedogenetic  
649 processes combined from all four distances from the drain. Error bars indicate 2SD between the  
650 four positions. Different superscript letters indicate significant differences in  $\delta^{65}\text{Cu}$  values among  
651 soil volumes according to ANOVA with Tukey's HSD taking the four distances from the drain  
652 as replicates.

653 Fig. 7. Mechanistic model of the fate of Cu in the drained Retisol. The size of the arrows indicate  
654 the dimension of Cu mass fluxes and the ‰ values refer to  $\Delta^{65}\text{Cu}_{\text{process-bulk soil}}$  values caused by  
655 the various processes.

656

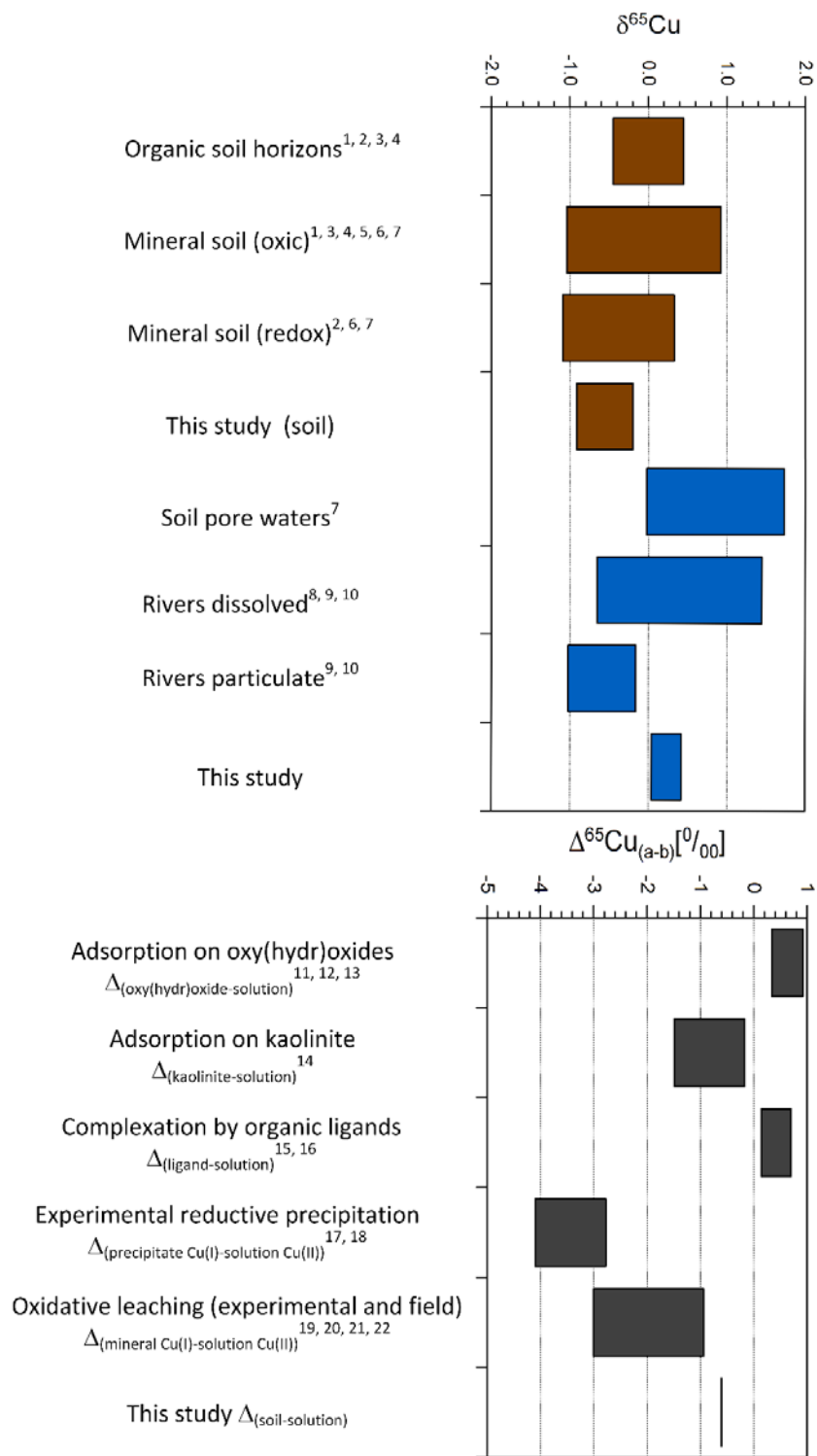
657

658



659

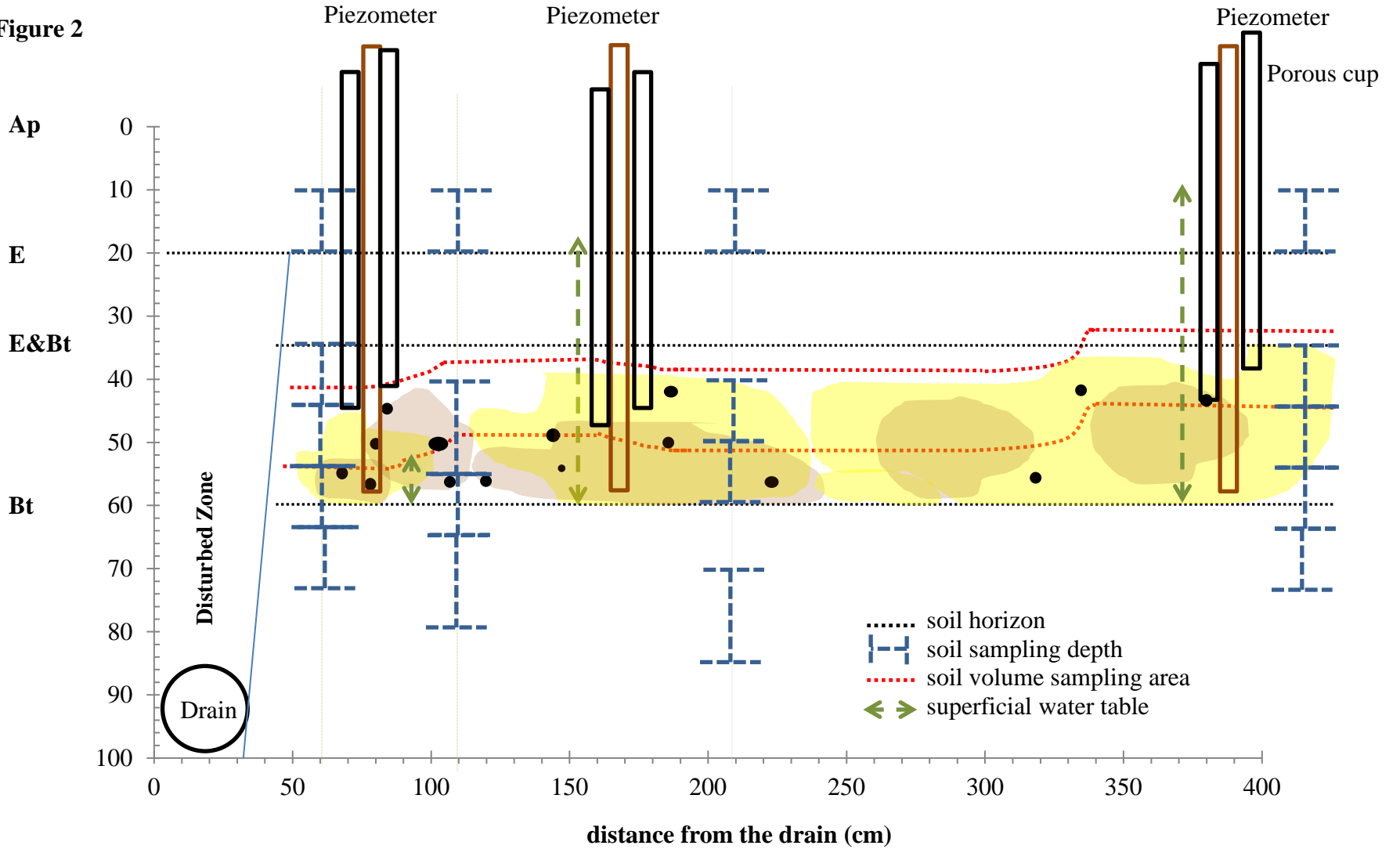
660 **Figure 1**



661

662

663 **Figure 2**

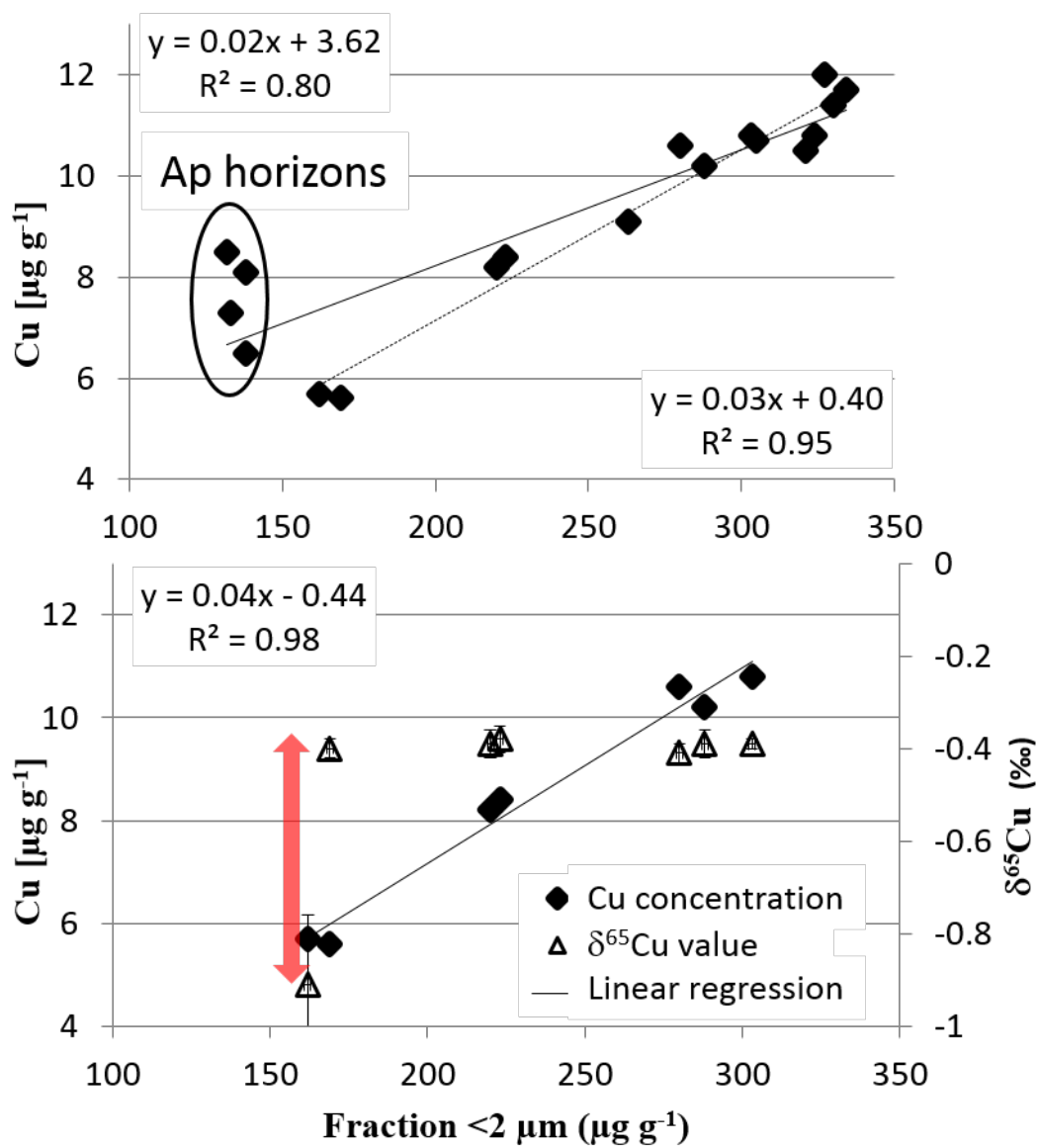


664

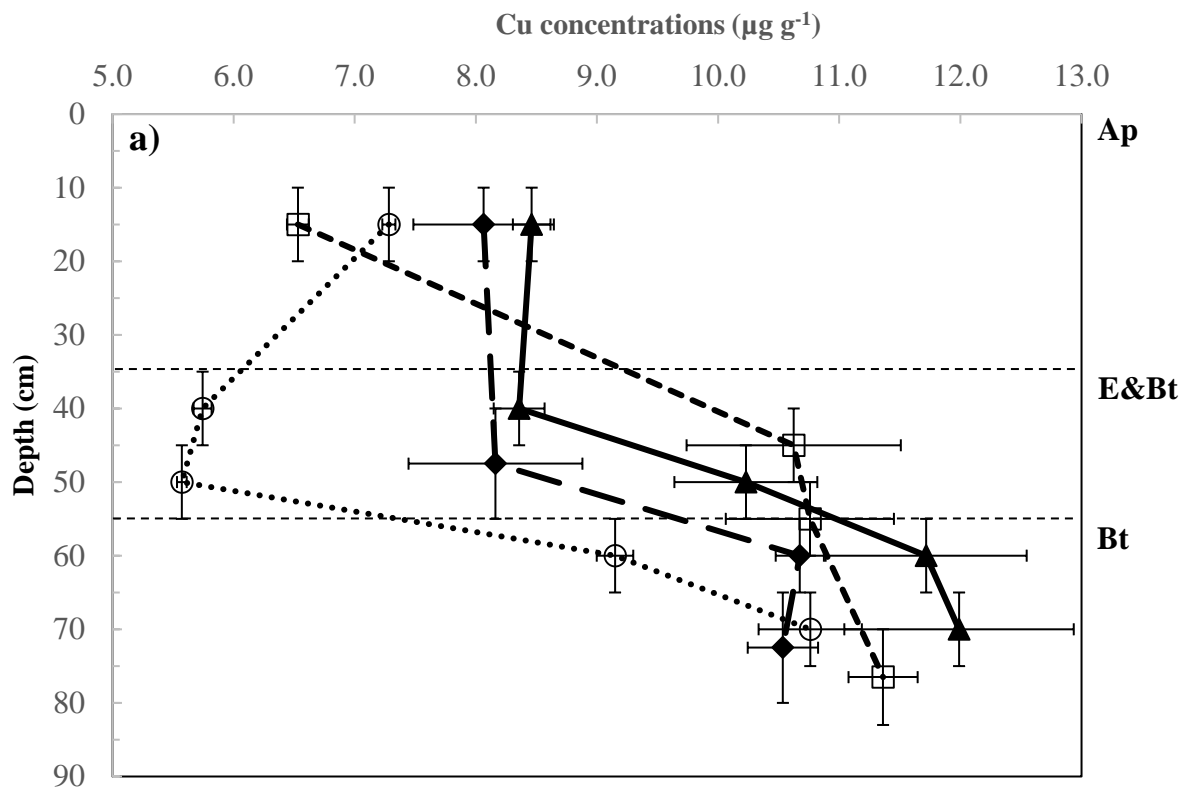
665

Figure 3

666



667

668 **Figure 4**

669

670

671

672

673

674

675

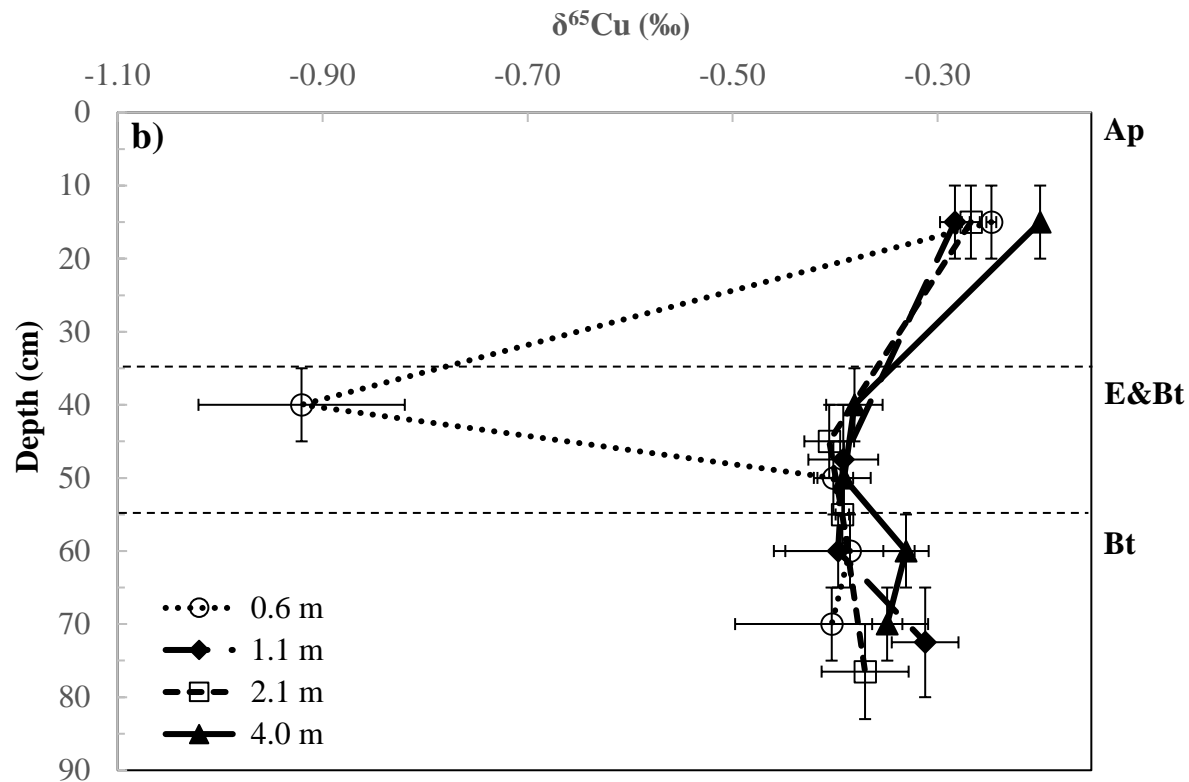
676

677

678

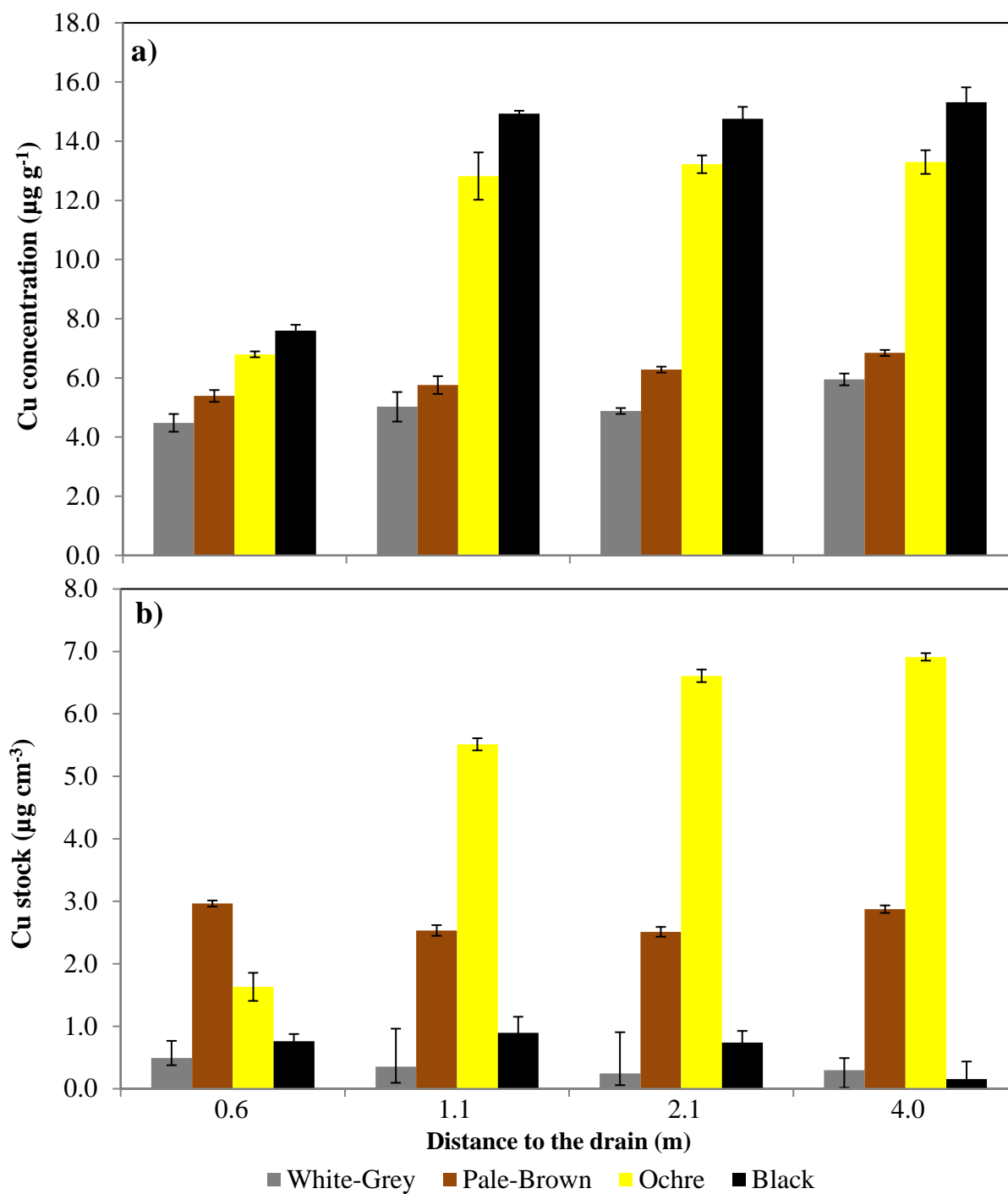
679

680



681

Figure 5



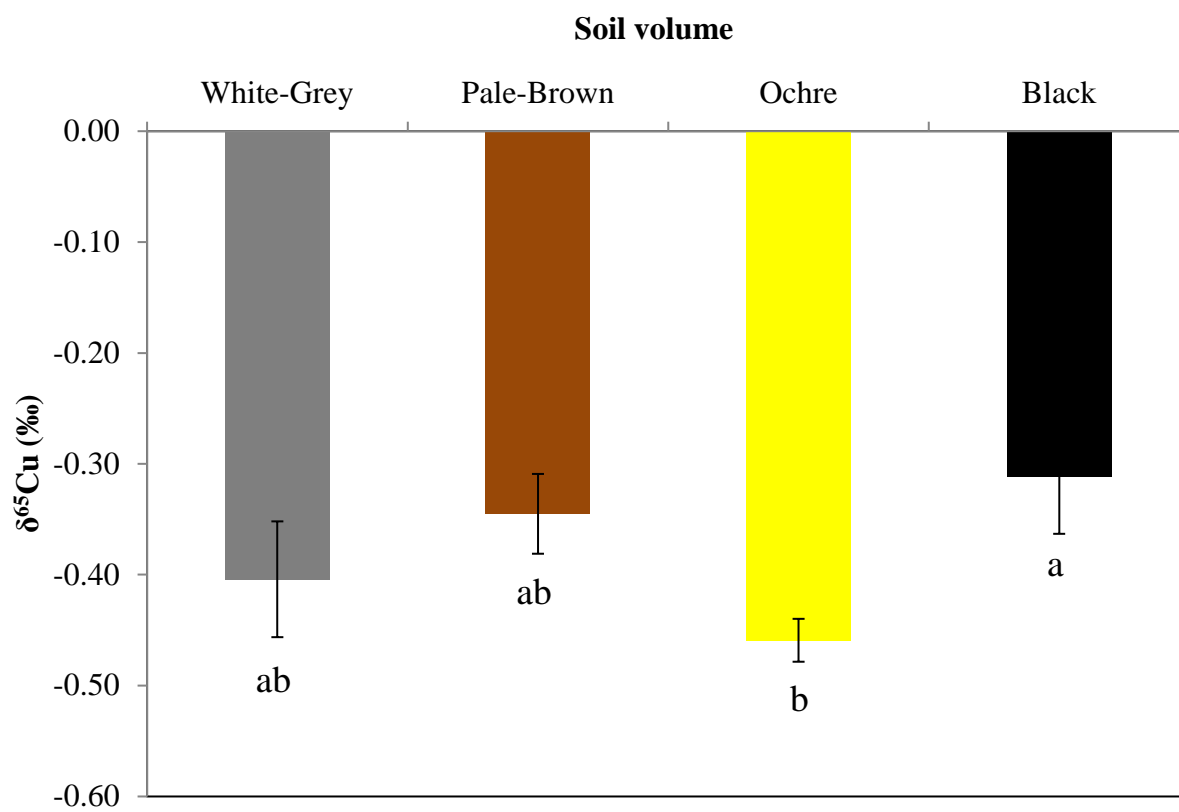
682

683

684

685

Figure 6



686

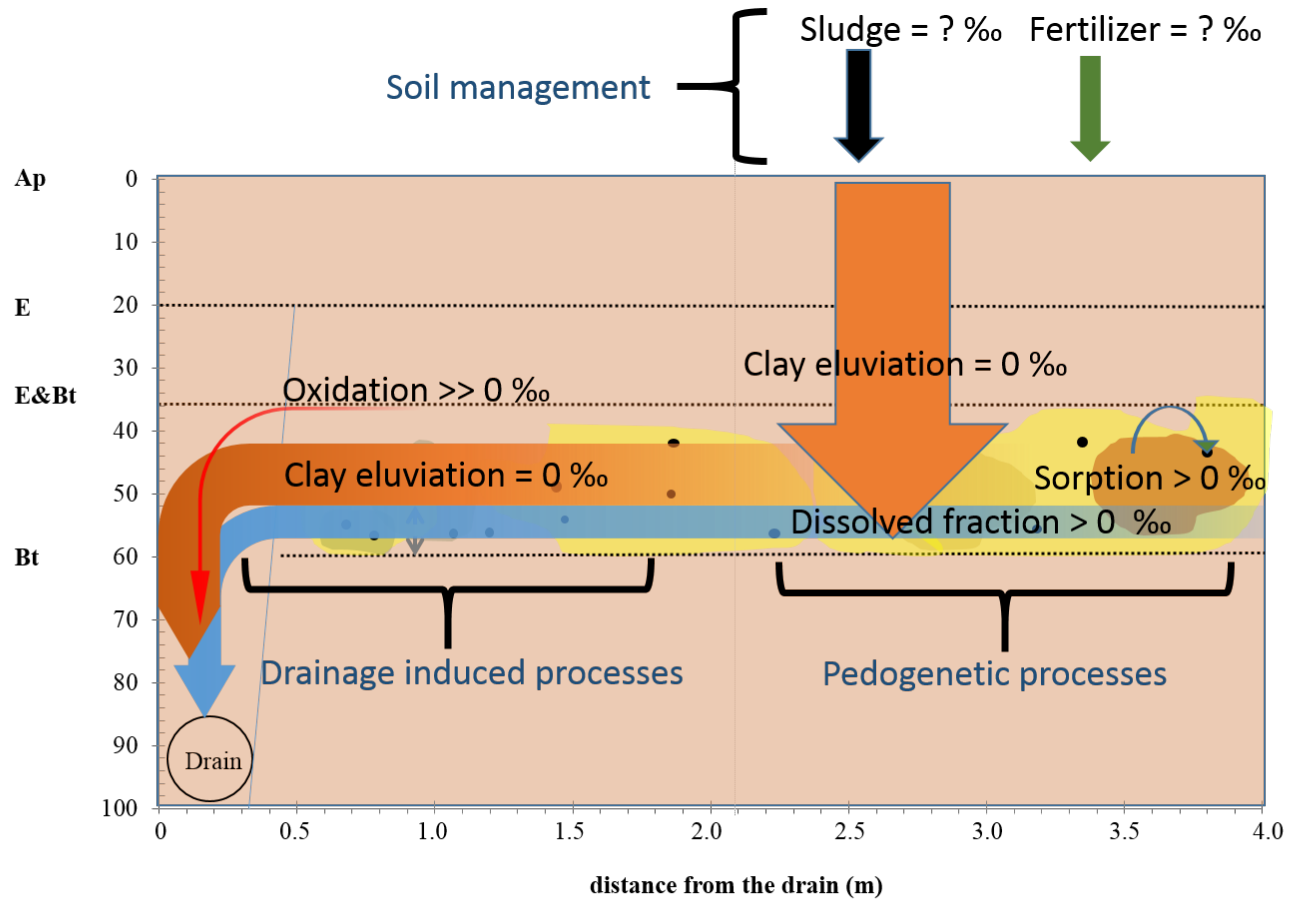
687

688

689

690

Figure 7



691

692